Chinese Chemical Letters 34 (2023) 107915

Contents lists available at ScienceDirect

Chinese Chemical Letters

journal homepage: www.elsevier.com/locate/cclet

Tetrapeptide self-assembled multicolor fluorescent nanoparticles for bioimaging applications

Yuerong Wang, Yang Lei, Jiaye Wang, Hui Yang*, Leming Sun*

School of Life Sciences, Key Laboratory of Space Bioscience & Biotechnology, Northwestern Polytechnical University, Xi'an 710072, China

ARTICLE INFO

Article history:
Received 13 August 2022
Revised 12 October 2022
Accepted 17 October 2022
Available online 19 October 2022

Keywords:
Self-assembly
Tetrapeptide
Multicolor
Fluorescent nanoparticles
Bioimaging

ABSTRACT

The biocompatibility and biodegradability of peptide self-assembled materials makes them suitable for many biological applications, such as targeted drug delivery, bioimaging, and tracking of therapeutic agents. According to our previous research, self-assembled fluorescent peptide nanoparticles can overcome the intrinsic optical properties of peptides. However, monochromatic fluorescent nanomaterials have many limitations as luminescent agents in biomedical applications. Therefore, combining different fluorescent species into one nanostructure to prepare fluorescent nanoparticles with multiple emission wavelengths has become a very attractive research area in the bioimaging field. In this study, the tetrapeptide Trp-Trp-Trp-Trp (WWWW) was self-assembled into multicolor fluorescent nanoparticles (TPNPs). The results have demonstrated that TPNPs have the blue, green, red and near infrared (NIR) fluorescence emission wavelength. Moreover, TPNPs have shown excellent performance in multicolor bioimaging, biocompatibility, and photostability. The facile preparation and multicolor fluorescence features make TPNPs potentially useful in multiplex bioanalysis and diagnostics.

Peptide self-assembled materials have attracted great interest in biomedical applications, due to its biocompatibility, biodegradability, intrinsic fluorescence, and flexible modulation [1–3]. Self-assembly of peptides is a spontaneous thermodynamic and kinetic driven process, which is mainly based on the intermolecular non-covalent interactions like hydrogen bonding, π-π stacking, electrostatic, hydrophobic, and van der Waals interactions [4–6]. Peptides can self-assemble into a variety of nanostructures, such as nanoparticles, nanotubes, nanobelts and nanofibers [7–10]. Based on these properties of peptide self-assembly, its applications in biomedical field have been extremely broadened. For example, autophagy-inducing peptide Beclin-1 (Bec1) was self-assembled into micelle-like nanoparticles (P-Bec1), which could effectively induce autophagy and inhibit the growth of tumors [11]. L-diphenylalanine (FF-MTs) was self-assembled into nanotubes that can be applied to drug delivery, especially for the delivery of a hydrophilic compound [12]. The cyclic peptide (L-histidine-D-histidine) can self-assemble into peptide material with the high-fluorescence efficiency [2]. However, conventional peptide self-assembly requires complex modification of peptides to achieve specific functions. Therefore, we have developed a universal peptide self-assembly strategy regulated by metal ion coordination, which could utilize peptides without additional modifications to explore their fluorescence properties [13–18].

In our previous work, tryptophan–phenylalanine self-assembled dipeptide nanoparticles (DNPs) with blue fluorescence were synthesized. DNPs can shift the peptide's intrinsic fluorescent signal from the ultraviolet fluorescence region to the blue fluorescence region (423 nm). It has been proved that DNPs could be used for bioimaging and real-time monitoring of drug release [13]. After that, in order to verify the universality of the peptide self-assembly strategy regulated by metal ion coordination, fluorescent cyclic peptide nanoparticles (f-PNPs) were self-assembled for the treatment of esophageal cancer [19]. The antitumor dipeptide carnosine could self-assemble into fluorescent carnosine nanoparticles (f-Car NPs), which have near-infrared (NIR) fluorescence emission and can be used for *in vivo* bio-imaging. Moreover, F-Car NPs also has the ability to enhance anti-tumor efficiency and biostability of carnosine [14]. These studies mainly focused on monochromatic fluorescent nanomaterials, which have limitations for biomedical applications due to unpredictable factors such as biological background fluorescence, instrumental efficiency, and environmental conditions [20–24]. Multicolor fluorescent nanomaterials such as semiconductor quantum dots, polymer dots, and organic fluorescent dyes can display multi distinguishable emission signals [25–28]. However, the potential of high toxicity, photobleaching and complex preparation process have hampered their practical appli-

* Corresponding authors.
E-mail addresses: kittyyh@nwpu.edu.cn (H. Yang), lmsun@nwpu.edu.cn (L. Sun).

https://doi.org/10.1016/j.cclet.2022.107915
1001-8417/

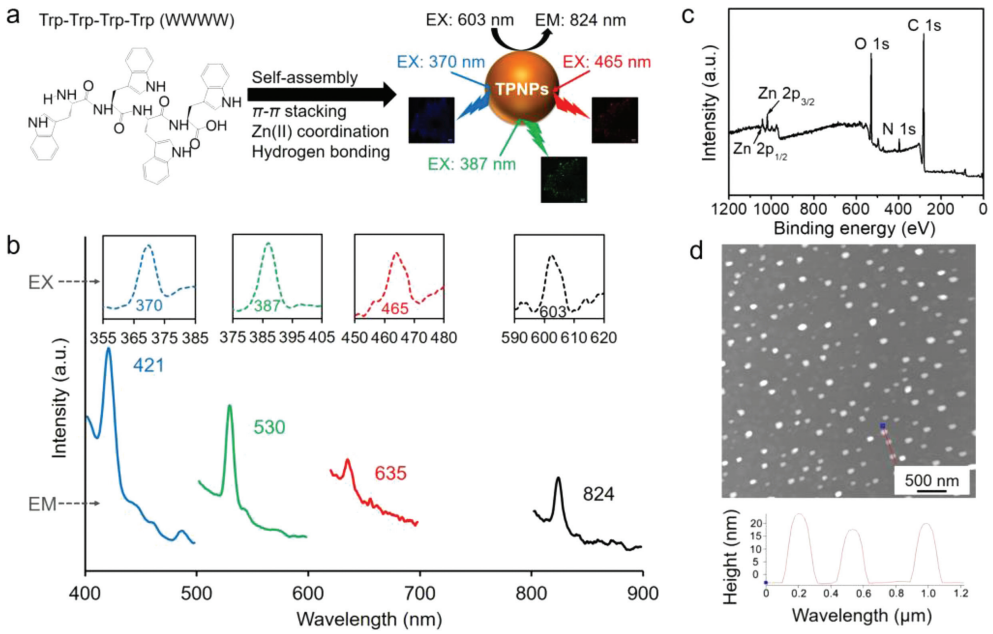

Fig. 1. Design and synthesis of TPNPs. (a) WWWW was self-assembled with Zn(II) to construct TPNPs through π-π stacking, zinc coordination and hydrogen bonding. (b) Multicolor fluorescence emission spectra of TPNPs. (c) XPS survey spectrum of TPNPs. (d) AFM image of TPNPs.

cations [29–32]. Because of the great biocompatibility and photostability, peptide self-assembled fluorescent nanomaterials have attracted much attention in recent years [15,33–35].

In this study, peptide nanoparticles with multicolor fluorescence were self-assembled successfully. Tetrapeptide Trp-Trp-Trp-Trp (WWWW) was self-assembled into multicolor fluorescent nanoparticles (TPNPs) through π-π stacking, Zn(II) coordination, and hydrogen bonding. The morphological and optical properties, as well as the biosafety of self-assembled TPNPs were characterized. The results showed that TPNPs possess blue (421 nm), green (530 nm), red (635 nm), and NIR (824 nm) fluorescence emission wavelength. TPNPs also have the ability for multiple fluorescent imaging of MCF-7 breast cancer cells *in vitro*. Moreover, TPNPs showed excellent performance in biocompatibility and photostability, which would raise the accuracy and reliability for biological analysis and detection.

Detailed experiment procedures are shown in supplementary material. According to previous reports, the π-π stacking interaction can provide a driving force for peptide self-assembly [13,36,37]. Peptides and Zn(II) have high binding affinity, and zinc ions can enhance the fluorescence emission [38,39]. Moreover, hydrogen bonding can promote the reaction of peptide self-assembly [40]. Therefore, in this study, tetrapeptide WWWW and Zn(II) self-assembled into multicolor fluorescent nanoparticles TPNPs through π-π stacking, Zn(II) coordination, and hydrogen bonding (Fig. 1a). After the self-assembly process, the size distribution of the self-assembled TPNPs were characterized by atomic force microscopy (AFM). The results demonstrated that TPNPs with an average diameter of 25 nm (Fig. 1d). Dynamic light scattering (DLS) experiment also revealed that the size of TPNPs was around 25 nm (Fig. S1 in Supporting information), which is consistent with the results of AFM. Then, the composition of the TPNPs were analyzed by X-ray photoelectron spectroscopy (XPS). The characteristic peaks related to Zn $2p_{1/2}$, Zn $2p_{3/2}$, O 1s, N 1s, and C 1s could be detected in the XPS spectrum of the TPNPs, which implied that the zinc ions coordinated with WWWW successfully. Furthermore, according to the structure of WWWW and the quantitative results of XPS, the ratio of zinc ions and WWWW within the TPNPs was about 1:1 (Fig. 1c and Table S1 in Supporting information).

The optical properties of TPNPs were characterized by fluorescent emission spectra and confocal images. The results showed that TPNPs have multicolor fluorescence emission properties. The spectral range of TPNPs covered the blue, green, red and NIR emission wavelengths (Fig. 1b). With the 370 nm excitation wavelength, TPNPs showed blue fluorescent with emission wavelength around 421 nm. Under the excitation wavelength of 387 nm, the fluorescence emission of TPNPs is about 530 nm, which is a green light in the visible light range. Under the excitation wavelength of 465 nm, the fluorescence emission of TPNPs is about 635 nm with a red light. With the 603 nm excitation wavelength, TPNPs showed NIR fluorescent with emission wavelength around 824 nm. The benzene rings of tryptophan can occur π-π stacking interaction, which is the driving force for the self-assembly process. The π-π stacking interactions can also reduce the excited state energy and increase the excitation and emission wavelengths, thus shifting the peptide's intrinsic ultraviolet fluorescence signal to the visible range and promote the self-assembly [14]. The zinc ions coordination can reduce fluorophore mobility and limit the energy dissipation through thermal relaxation pathways for better fluorescence intensity [13]. In addition, WWWW has straight and long chain, which structure is more flexible that have more possibilities to produce different structures through self-assembly for multicolor fluorescence. More intuitively, the aggregated TPNPs showed clear blue, green, and red colors using the confocal microscope (Fig. S2 in Supporting information). The fluorescent images also showed the similar multicolor properties. The multicolor fluorescence property of TPNPs could reveal the exact location, number and state of cells, which can improve the accuracy of biological analysis and detection.

Organic fluorescent dyes DAPI, Rh6G, RhB and ICG were utilized to test the photostability of TPNPs (Fig. S3 in Supporting information). All of the selected organic fluorescent dyes have the corresponding fluorescence to the TPNPs with different emission wavelengths. The photostability were investigated by the fluorescence emission spectrum of TPNPs. The comparative tests of TPNPs and DAPI with 421 nm emission wavelength (Fig. S3a), TPNPs and Rh6G with 530 nm emission wavelength (Fig. S3b), TPNPs and RhB with 635 nm emission wavelength (Fig. S3c), TPNPs and

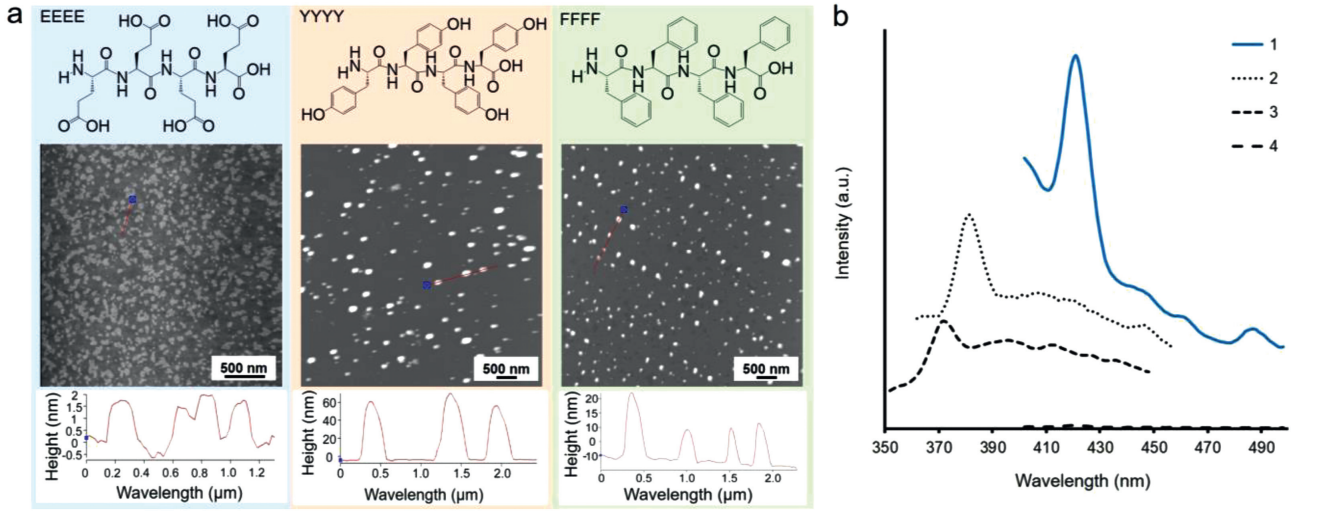

Fig. 2. The effects of peptide sequences on the fluorescent properties. (a) AFM results of tetrapeptides EEEE, YYYY and FFFF self-assembled materials. (b) The fluorescence emission spectra of tetrapeptides self-assembled materials: WWWW (1), YYYY (2), FFFF (3), and EEEE (4) self-assembles.

ICG with 824 nm emission wavelength (Fig. S3d) showed that after continuous irradiation for 120 s, the fluorescence intensity of TPNPs remained stable. However, the fluorescence intensity of all the corresponding organic dyes decreased accordingly. This result indicated that TPNPs have a better photostability compared with organic fluorescent dyes. The optical properties of TPNPs demonstrated that TPNPs not only have multicolor fluorescence, but also have a high photostability, highlighting its potential for bioimaging. Furthermore, the stability of TPNPs in DI water, PBS, and culture medium was tested (Fig. S4 in Supporting information). After 24 h, the fluorescence still could be observed and the relative intensity were all higher than 50%. The result showed that the structure of TPNPs is stable.

To get a deeper insight of the self-assembly process, tetrapeptides Tyr-Tyr-Tyr-Tyr (YYYY), Phe-Phe-Phe-Phe (FFFF) and Glu-Glu-Glu-Glu (EEEE) were self-assembled under same experimental conditions (Fig. 2). The π-π stacking interaction between the benzene rings is the driving force for the self-assembly process [13]. So, the tetrapeptides of two other amino acids with benzene rings YYYY and FFFF were chosen as controls. Moreover, EEEE without benzene ring was also selected as control, which could reveal the importance of π-π stacking in the process of peptide self-assembly. According to the AFM images and diameter analysis, the tetrapeptide EEEE cannot self-assemble into nanoparticles, tetrapeptides YYYY and FFFF can successfully self-assemble into nanoparticles. The diameter of YYYY and FFFF self-assembled nanoparticles are around 60 nm and 10-30 nm respectively (Fig. 2a). EEEE has no benzene ring in its structure, but YYYY and FFFF have benzene rings, which indicates that the π-π stacking between benzene rings can serve as a driving force for self-assembly. After that, the fluorescent properties of those three samples were also obtained. EEEE self-assembles have no fluorescent properties. YYYY and FFFF self-assembles only have fluorescent emission in UV ranges. Both of them do not have any other fluorescent colors like WWWW self-assembles (Fig. 2b). Compared to the other three amino acids, tryptophan has long emission wavelength and high quantum yield [13], so WWWW self-assembled nanoparticles TPNPs have excellent fluorescence properties.

The effects of reaction conditions on self-assembly process were studied with fluorescence emission spectra (Fig. 3). As control, the experiment with Zn(II) at room temperature and without Zn(II) at room temperature were also established. According to the results, under the excitation wavelength of 370 nm, the fluorescence emission peak of WWWW self-assembly with Zn(II) after heating is about 421 nm, which has an obvious higher fluorescence intensity. However, both of the control groups WWWW self-assembly with Zn(II) at room temperature and without Zn(II) at room temperature showed a very low fluorescence emission peak (Fig. 3a). Similarly, under the excitation wavelength of 387 nm (Fig. 3b), 465 nm (Fig. 3c) and 603 nm (Fig. 3d), the similar results were obtained. Furthermore, at these three emission wavelengths, WWWW self-assembly without Zn(II) at room temperature almost have no fluorescence. It can be concluded that Zn(II) coordination and heating are necessary for the self-assembly of TPNPs. Zn(II) has high polarizability so that it can form a rigid chelate structure with the peptide. Furthermore, the Zn(II) rigid chelate structure reduces fluorophore mobility, which can limit the energy dissipation during thermal relaxation pathways and obtain better quantum yield and fluorescence intensity. In addition, after heating, the reaction system becomes more active, which speeds up the movement of the molecules and further speeds up self-assembly. Therefore, WWWW self-assembly with Zn(II) under heat is the optimal condition for synthesizing TPNPs.

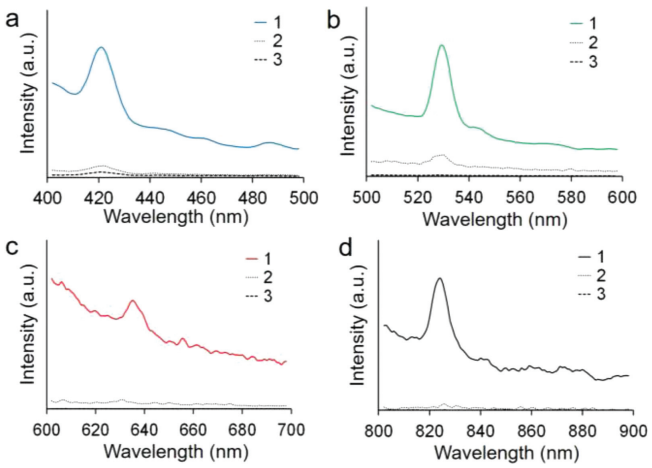

Fig. 3. Optical characterizations of TPNPs. The emission wavelength of TPNPs synthesized under different conditions at an excitation wavelength of 370 nm (a), 387 nm (b), 465 nm (c) and 603 nm (d): (1) WWWW self-assembly with Zn(II) after heating, (2) WWWW self-assembly with Zn(II) at room temperature, (3) WWWW self-assembly without Zn(II) at room temperature.

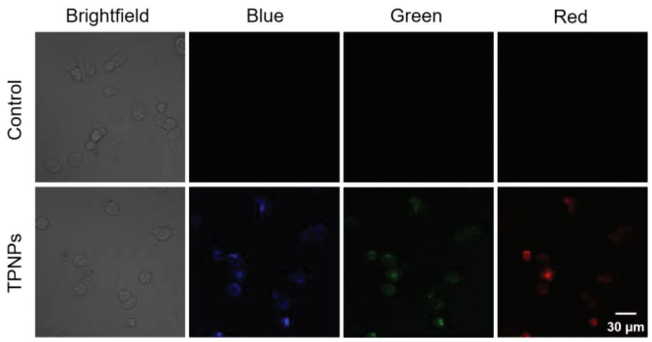

Fig. 4. Confocal fluorescence images of MCF-7 cells incubated with TPNPs after 3 h. The excitation wavelengths are 370 nm (blue fluorescence), 387 nm (green fluorescence) and 465 nm (red fluorescence).

To monitor the multicolor bioimaging properties of TPNPs, the confocal fluorescence cellular imaging of MCF-7 breast cancer cells incubated with TPNPs *in vitro* were conducted (Fig. 4). After 3 h incubation, TPNPs showed multicolor fluorescence emission at different wavelengths of excitation. When the TPNPs were excited at 370, 387 and 465 nm, the corresponding multicolor fluorescence was clearly observed in the blue (421 nm), green (530 nm) and red (635 nm) channels, respectively. However, the control group did not display any fluorescence signal. This result demonstrated that the multicolor fluorescence characteristic of TPNPs may find potential applications in multiplex bioassays without complex instrumentation and processing. Generally, monochromatic fluorescent nanomaterials have limitations in biomedical applications, due to the factors such as biological background fluorescence, instrumental efficiency, and environmental conditions. Thus, this multicolor fluorescent imaging could avoid these unpredictable factors.

Toxicity is a major consideration in biological applications. In this case, the cytotoxicity of TPNPs was determined by cell culture using HaCaT cells. The cell counting assay kit-8 (CCK-8) assay was used to evaluate the viability of HaCaT cells after exposure to the TPNPs for 24 h at various concentrations (10-50 μg/mL) (Fig. S5 in Supporting information). Over 90% cell viability is observed after incubation of HaCaT cells with TPNPs, and there are no significant changes in viability values compared the evaluated groups with the control group, which indicate that TPNPs possess excellent biocompatibility. These data revealed that TPNPs would have great benefits for biomedical applications, especially for practical imaging applications.

In summary, we report the synthesis of multicolor fluorescent nanoparticles (TPNPs) through π-π stacking, Zn(II) coordination and hydrogen bonding. Tryptophan has long emission wavelength and the structure of WWWW is more flexible, thus it is more possible to produce multicolor fluorescence through self-assembly. TPNPs have blue (421 nm), green (530 nm), red (635 nm), and NIR (824 nm) emission wavelength. Compared with the organic fluorescent dyes DAPI, Rh6G, RhB and ICG, TPNPs have a better photostability. Moreover, TPNPs exhibit excellent multicolor cellular imaging capability, good biocompatibility, and almost have no toxic effect on cells. In conclusion, the multicolor fluorescence characteristic, photostability and biocompatibility of the TPNPs make them highly suitable for bioimaging and have potential applications in multiplexed bioimaging and bioanalysis.

Declaration of competing interest

The authors declare that they have no known competing financial interests or personal relationships that could have appeared to influence the work reported in this paper.

Acknowledgments

This work was supported by the National Natural Science Foundation of China (No. 31900984), the Fundamental Research Funds for the Central Universities (No. D5000210899), and Innovation and Entrepreneurship Fund from the Student Affairs Department of the Party Committee of Northwestern Polytechnic University (No. 2021-CXCY-019).

Supplementary materials

Supplementary material associated with this article can be found, in the online version, at doi:10.1016/j.cclet.2022.107915.

References

[1] E. Busseron, Y. Ruff, E. Moulin, N. Giuseppone, Nanoscale 5 (2013) 7098–7140.
[2] Y. Chen, A.A. Orr, K. Tao, Z.B. Wang, et al., ACS Nano 14 (2020) 2798–2807.
[3] L.L. Zhao, Y.L. Xing, R. Wang, et al., ACS Appl. Bio. Mater. 3 (2020) 86–106.
[4] L. Sun, A. Li, Y. Hu, et al., Part. Part. Syst. Charact. 36 (2019) 1800420.
[5] J. Wang, K. Liu, R.R. Xing, X.H. Yan, Chem. Soc. Rev. 45 (2016) 5589–5604.
[6] D.C. Liu, D.J. Fu, L.B. Zhang, L.M. Sun, Chin. Chem. Lett. 32 (2021) 1066–1070.
[7] S. Chen, Y.Z. Liu, R. Liang, et al., Chin. Chem. Lett. 32 (2021) 3903–3906.
[8] Q.B. Meng, Y.Y. Kou, X. Ma, et al., Langmuir 28 (2012) 5017–5022.
[9] Y.X. Li, L.Y. Yan, K. Liu, et al., Small 12 (2016) 2575–2579.
[10] N. Habibi, N. Kamaly, A. Memic, H. Shafiee, Nano Today 11 (2016) 41–60.
[11] Y. Wang, Y.X. Lin, Z.Y. Qiao, et al., Adv. Mater. 27 (2015) 2627–2634.
[12] R.F. Silva, D.R. Araujo, E.R. Silva, et al., Langmuir 29 (2013) 10205–10212.
[13] Z. Fan, L.M. Sun, Y.J. Huang, et al., Nat. Nanotechnol. 11 (2016) 388–394.
[14] W. Lin, Y. Yang, Y. Lei, et al., ACS Appl. Mater. Interfaces 13 (2021) 32799–32809.
[15] D.J. Fu, D.C. Liu, L.B. Zhang, L.M. Sun, Chin. Chem. Lett. 31 (2020) 3195–3199.
[16] L.M. Sun, Y. Lei, Y.R. Wang, D.C. Liu, Chin. Chem. Lett. 33 (2022) 1946–1950.
[17] L.M. Sun, D.C. Liu, D.J. Fu, et al., Chem. Eng. J. 405 (2021) 126733.
[18] L.M. Sun, Z. Fan, T. Yue, et al., Bio-Des. Manuf. 1 (2018) 182–194.
[19] Z. Fan, Y. Chang, C.C. Cui, et al., Nat. Commun. 9 (2018) 3217.
[20] J. Kong, J.X. Zhang, Y.F. Wang, et al., ACS Appl. Mater. Interfaces 12 (2020) 31830–31841.
[21] J. Liu, J. Liu, W.S. Liu, et al., Inorg. Chem. 54 (2015) 7725–7734.
[22] X.C. Liu, J.B. Fei, A.H. Wang, et al., Angew. Chem. Int. Ed. 56 (2017) 2660–2663.
[23] K. Tao, P. Makam, R. Aizen, E. Gazit, Science 358 (2017) eaam9756.
[24] Y.Q. Yan, H. Wang, Y.L. Zhao, Chin. Chem. Lett. 33 (2022) 3361–3370.
[25] J. Chen, P.S. Zhang, G. Fang, et al., J. Phys. Chem. B 116 (2012) 4354–4362.
[26] G. Gao, Y.W. Jiang, W. Sun, F.G. Wu, Chin. Chem. Lett. 29 (2018) 1475–1485.
[27] S. He, Q.T. Huang, Y. Zhang, et al., Chin. Chem. Lett. 32 (2021) 1462–1465.
[28] X. Geng, Y.Q. Sun, Z.H. Li, et al., Small 15 (2019) 1901517.
[29] Y.C. Wang, R. Hu, G.M. Lin, et al., ACS Appl. Mater. Interfaces 5 (2013) 2786–2799.
[30] Y. Rong, C.F. Wu, J.B. Yu, et al., ACS Nano 7 (2013) 376–384.
[31] D.D. Yao, S.S. Zhao, J.H. Guo, et al., J. Mater. Chem. 21 (2011) 3568–3570.
[32] K. Jiang, S. Sun, L. Zhang, et al., Angew. Chem. Int. Ed. 54 (2015) 5360–5363.
[33] K.N. Wang, W. Ma, Y.C. Xu, et al., Chin. Chem. Lett. 31 (2020) 3149–3152.
[34] F. Yang, D. Zhang, Q.M. Zhou, et al., Chin. Chem. Lett. 33 (2022) 2901–2905.
[35] X.K. Chen, X.D. Zhang, F.G. Wu, Chin. Chem. Lett. 32 (2021) 3048–3052.
[36] J.J. Panda, V.S. Chauhan, Polym. Chem. 5 (2014) 4418–4436.
[37] C.H. Chen, X.H. Ji, Chin. Chem. Lett. 29 (2018) 1287–1290.
[38] K. Tao, Y. Chen, A.A. Orr, et al., Adv. Funct. Mater. 30 (2020) 1909614.
[39] X.X. Shi, P. Yang, X.F. Peng, et al., Polymer 170 (2019) 65–75.
[40] J. Kang, D. Miyajima, T. Mori, et al., Science 347 (2015) 646–651.